verification, qualification, factory acceptance, integrated systems, and prelaunch and postlaunch tests. The planning goal should be to insure that all hardware is qualified for all environments encountered throughout the duration of the mission with the minimum expenditure of program funds, time, and manpower.

2) To be cost effective, the test-program planning must be initiated early in the design-requirements phase to permit sufficient time to conduct tradeoffs for alternate designs against later requirements for testing. Long life in the equipment must be considered as a design function, supported by inflight maintenance when practical, rather than as the purpose of the test program. An excellent paper presented by R. W. Lanzkron to the AIAA covers this subject.[6]

3) A broad trade-off study should be employed to reach a balance between testing, analysis, and design. This study should make full use of the test data and the results of past programs. Life and failure histories of systems and components proposed for use in the current program should be included in the total tradeoff study.

4) The utilization of interface-simulation devices should be considered in the development of test programs for long-duration orbital missions. This recommendation is made based upon the increased size and complexity of the flight modules as well as upon the absence for ground checkout of actual flight-module interfaces after the modules are in orbit. Associated with this recommendation is the need for a high level of configuration-control management of the flight interfaces and the corresponding simulators to insure proper mating during the mission.

References

[1] Allen, W. R., "Accelerated Life Tests of Items with Many Modes of Failure," TR 44 (U.S. Army Contract DA-034-ORD-2297), Feb. 1962, Princeton Univ., Princeton, N. J.

[2] "Dynamic Mission Equivalent Test Analysis of the Mariner Venus '67 Spacecraft," Doc. 68SD4297, Aug. 1968, General Electric Co., Valley Forge, Pa.

[3] Charp, S., "Test and Evaluation Aspects of the Nimbus II Program Useful to Other Long Life Space Programs," *Proceedings of the Canaveral Council of Technical Societies 5th Space Congress*, Vol. 2, Mar. 1968, pp. 17.1-1–17.1-16.

[4] "Apollo Spacecraft Test Engineering Certification Test Program Guidelines," MSC Doc. MSC-ASPO-RQA-11A, Jan. 1967, NASA; supersedes ASPO-RQA-11, May 1965.

[5] Westerheid, R. J., "The Apollo Spacecraft Qualification Program," *Annals of Assurance Sciences; Proceedings of the AIAA/ASME 8th Reliability and Maintainability Conference*, July 1969, pp. 153–159.

[6] Lanzkron, R. W., "Maintenance of Future Spacecraft in Orbit," AIAA Paper 68-1060, Philadelphia, Pa., 1968.

DECEMBER 1970 J. SPACECRAFT VOL. 7, NO. 12

Ablative Material Response to CO_2 Laser Radiation

WILLIAM D. BREWER*
NASA Langley Research Center, Hampton, Va.

Results are presented from an experimental study to evaluate the performance of various ablative materials subjected to radiative heat fluxes in the range 36–47 Mw/m². The radiative environment was produced by a 9-kw, continuous-wave CO_2 laser. Carbon-phenolic, phenolic-nylon, a filled epoxy material in honeycomb (Apollo material), and graphite were tested in air, nitrogen, and helium at pressures of 1.0, 0.3, and 0.1 atm. A silicone elastomer and a polybenzimidazole (PBI) were tested in air and nitrogen at 0.1 atm. The behavior of the ablative materials was relatively insensitive to changes in test gas, pressure, and heat flux. The PBI and phenolic-nylon withstood the severe environment reasonably well, whereas the elastomer and the epoxy material showed large surface recession, and the carbon-phenolic was subject to considerable spallation, apparently due to thermal stresses within the material. The graphite, tested primarily for reference purposes, showed improvement in performance with increasing heat flux and showed little effect of changes in environmental pressure over the range considered.

Introduction

THE performance of ablative materials subjected to environments such as those encountered in Earth re-entry at orbital and escape velocity has been extensively investigated, and analyses have been developed with which the behavior of materials in such environments can be satisfactorily predicted (see, e.g., Ref. 1). For proposed interplanetary missions, however, the heating will be much more severe. Because of the high entry velocities, atmospheric entry in such missions is characterized by large radiative heat inputs to an entry vehicle, typically in the range 30–50 Mw/m².[2] There is a need for a better understanding of the interaction of the high-radiative heating environments with thermal protection systems.

An experimental program was undertaken to obtain information about the behavior of the ablative materials subjected to large radiative heat fluxes. The only facilities presently available which are capable of producing the required level of radiant heating continuously are gas lasers. For this investigation a CO_2 laser capable of a maximum power output of about 9 kw was used.[3] This facility produces continuous radiation at 10.6 μm wavelength for run times up to several minutes.

The materials tested are representative of those commonly considered as candidate materials for re-entry vehicle thermal protection systems. They were tested in air, nitrogen, and

Presented as Paper 70-864 at the AIAA 5th Thermophysics Conference, Los Angeles, Calif., June 29–July 1, 1970; submitted August 3, 1970; revision received September 18, 1970.

* Aerospace Engineer, Thermal Analysis Section, Structures Research Division.

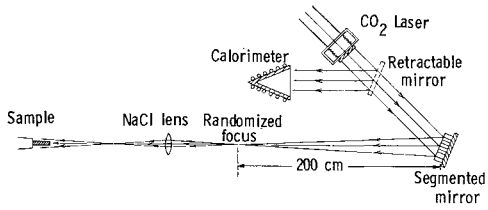

Fig. 1 Optical schematic for laser beam control.

helium at 1.0, 0.3, and 0.1 atm. The test samples were flat-faced cylinders, 0.64 cm in diameter. Heat fluxes to them were in the range 36–47 Mw/m². The materials were evaluated by an effectiveness parameter based on the measured depth of material degradation and visual observation of the material behavior.

Test Apparatus

All tests were made with the CO_2 laser at the Raytheon Company. This d.c.-excited, flowing-gas, CO_2-N_2-He laser is made up of 15 sections, each about 15 m long and connected optically to form a continuous device 225 m long. The maximum power output from all sections is about 9 kw. The design, construction, and operating characteristics of the laser are discussed in detail in Ref. 3.

For the present tests, the laser was operated at about 6 kw with a beam diameter of 4.4 cm. The beam emerges from the laser tube and is reflected by a "segmented mirror" through a lens onto the sample surface (Fig. 1). The segmented mirror is used to scramble the beam to obtain a more nearly uniform and stable power density across the surface of the sample. The mirror is a close-packaged array of circular flats, each 0.95 cm in diameter. The surfaces of the flats are set at angles to approximate a paraboloidal surface of 2 m focal length. Thus, after reflection from the mirror, the beam passes through a circle of minimum diameter (about 1.3 cm) at a point 2 m from the mirror surface. Because of the random interference effects produced by the segmented mirror, the intensity distribution at the focal plane is relatively insensitive to the distribution across the beam at the laser exit. The NaCl lens refocuses the beam at a point about 16 cm from the sample surface and hence produces a slightly divergent beam at the sample. A retractable mirror, pneumatically controlled, is used to switch the beam from the sample optics to a calorimeter for monitoring and calibrating the beam. The mirror is controlled by an electrical timer and is used to begin and terminate sample exposure to the laser beam.

The sample is enclosed in a four-port test chamber (Fig. 2). Glass windows on the two side ports permit observation of the sample during testing. Motion pictures and sample temperature measurements are made through these windows.

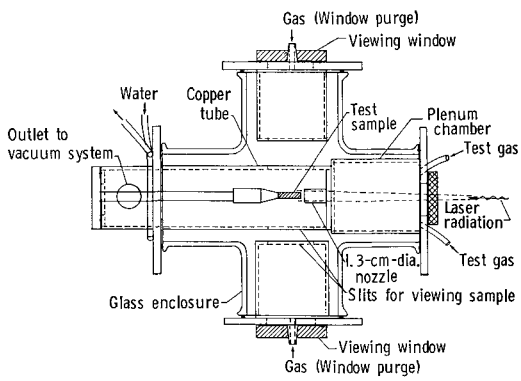

Fig. 2 Schematic diagram of test chamber.

The front port has a NaCl window through which the laser beam passes after traversing the optical system as shown in Fig. 1. The beam passes through a 1.3-cm-diam nozzle and impinges on the sample surface. The test gas is injected into a plenum chamber, passes through the nozzle, and flows past the sample. A vacuum system is connected at the rear of the chamber to remove the test gas as well as the ablation products and to control the pressure in the chamber. Gas is also injected into the side ports such that the flow is over the inside surface of the glass viewing windows. Thus, any ablation products which may not be immediately removed by the vacuum system are swept away from the window, and no clouding of the window results.

The rear port permits insertion of the sample into the test position. The sample is held in place by a conical, copper device which reflects the radiation not incident on the sample surface onto a water-cooled copper tube surrounding the sample. This inside of the tube is blackened to improve its absorptive characteristics.

Instrumentation and Calibration

The pressure inside the test chamber was measured with two gages, one calibrated for 0–0.3 atm and one for 0–1.0 atm. The pressure was controlled by the vacuum system. Standard, precision-bore flow meters were used to measure the gas flow rates into the plenum chamber; and into the side ports. Control valves were located appropriately so that the gas flow rates could be adjusted.

An optical pyrometer was used to measure the temperatures of the test samples, on the sides of the samples as near their front surfaces as possible. The pyrometer was calibrated to account for absorption of radiation from the sample by the glass window.

Power measurements were made with water-cooled calorimeters (Ref. 3). One calorimeter measured the total power of the laser beam as the beam emerged from the laser tube (see Fig. 1). A second calorimeter was placed at the rear port of the test chamber to determine the total power of the beam after the beam had been attenuated by the optical system. The intensity distribution across the beam at the test location was determined by exposing 1.2-cm-diam rods of polystyrene to the laser beam. The polystyrene has a low melting point and a very high-absorption coefficient at 10.6 μm. The rods were sectioned after a 0.5-1-sec exposure to the laser beam and the intensity profile was determined by the shape of the hole burned into the rods. The validity of this technique for determining the profile was checked by a point-by-point measurement of the power density across the diameter of the beam. A probe consisting of a 2.5-cm-diam tube to which was attached a hollow cone tapering from 2.5-cm-diam to 0.16-cm-diam was moved across the beam (see Fig. 3). A low-power radiometer was used to determine the power transmitted through this 0.16-cm-diam hole. These data agreed well with the results obtained with the polystyrene rods (Fig. 4), indicating that the polystyrene profile is a good representation of the actual intensity distribution. The system was calibrated so that only a mea-

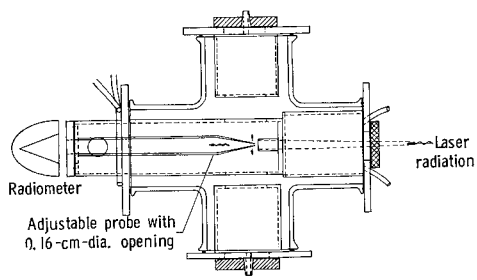

Fig. 3 Setup for beam intensity profile measurement.

surement of the beam power at the laser exit was required to determine the maximum heat flux to the sample and the heating distribution over the sample surface.

Samples, Test Conditions, and Procedures

The test samples were 0.64-cm-diam, flat-faced cylinders, 7.6 cm in length. They were positioned in a copper holder (Fig. 2) so that only about 3 cm extended out of the holder. The test materials were:

1) a carbon-phenolic composite, ~50% phenolic resin and 50% carbon fibers, with a density of ~1450 kg/m³;

2) a high-density phenolic nylon (HDPN), 50% phenolic resin and 50% nylon powder, 1200 kg/m³;

3) a low-density phenolic-nylon (LDPN), 25% phenolic resin, 25% phenolic Microballoons, and 50% nylon powder, 550 kg/m³;

4) a silicone elastomer, ~75% silicone resin, 15% SiO_2 in the form of tiny hollow spheres (11%) and fibers (4%), and 10% phenolic Microballoons (materials 1–4 are discussed in more detail in Refs. 4 and 5);

5) a filled epoxy material (Apollo material), whose composition is proprietary information, ~500 kg/m³ (some measured material properties are given in Ref. 4);

6) a polybenzimidazole (PBI), which is 69% PBI prepolymer, 13% carbon fibers, and 18% phenolic Microballoons, ~500 kg/m³ (material 5, Ref. 6); and

7) a commercial-grade, fine-grained graphite, 1800 kg/m³.

The silicone elastomer and the PBI material were tested in air and nitrogen at 0.1 atm. All other materials were tested in air, nitrogen, and helium at 0.1, 0.3, and 1.0 atm. Maximum heat fluxes ranged from 36 to 47 Mw/m. The heating was not uniform over the surface of the samples, however. The heat flux at the edge of the samples ranged from 70% to 85% of the maximum, depending upon the power output of the laser (see Fig. 4). The gas flow rates were small (~3 gm/sec) but were sufficient to remove the ablation products from the area of the test sample. The flow was subsonic (~30 m/sec), uniform over the surface of the samples, and stable throughout each test. To obtain significant recession, the graphite samples were tested for 5 sec; all others were tested for 2 sec.

The samples were placed in the test chamber, the appropriate gas was injected into the chamber, and the desired pressure was obtained by regulating the vacuum system. Then, the laser was brought up to the operating level with the retractable mirror reflecting the beam into the calorimeter (see Fig. 1). When the laser output had stabilized, the power output was recorded, the mirror was removed from the path of the beam, and the sample was exposed to the laser radiation for the prescribed length of time. At the end of the test, the mirror was again inserted into the path of the beam.

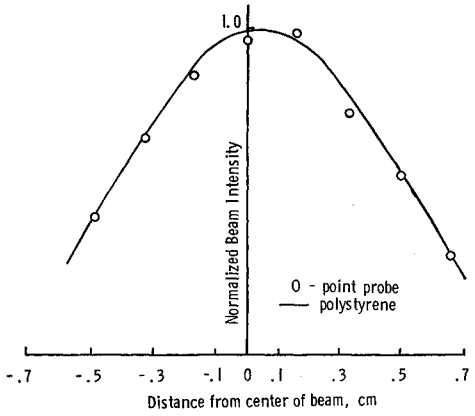

Fig. 4 Comparison of point-probe and polystyrene measurements of beam intensity profile.

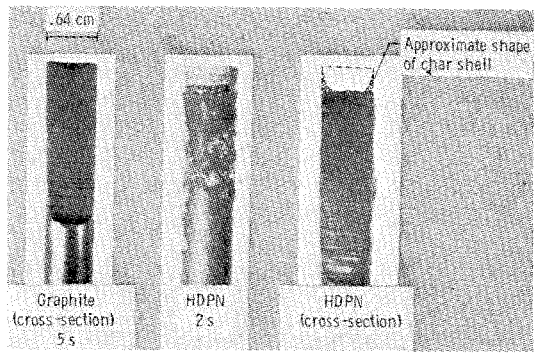

Fig. 5 Graphite and HDPN samples after testing in H_e at 1.0 atm.

Another power measurement was made to determine whether the laser output had changed during the test. Each sample was measured and weighed before and after testing to determine the surface recession and mass lost.

Results and Discussions

The emphasis of this experiment is on the ablative materials other than graphite, since graphite is not generally considered a prime contender for heat shields for manned re-entry vehicles. Some discussion of the graphite results is given, however.

Material Behavior

Post-test photographs of graphite and HDPN tested in helium at 1.0 atm are shown in Fig. 5. The front surface of the graphite is cupped slightly and has the same general shape as the heating distribution. A thin shell of charred material remained on the HDPN sample after testing. The height of the char shell is apparent in the center photograph in Fig. 5. The cross-section view of the sample shows the approximate shape of the char. The char shells were thin and fragile and in most cases broke or separated from the samples during handling. Over most of the surface the char layer was very thin and the interface between the char and the uncharred layer was flat rather than cupped, indicating that the interface was "seeing" a reasonably uniform heating environment. The sides of the models were apparently cooled sufficiently by reradiation to permit a considerable height of char to build up at the edges. For a given test gas, the height of the shells appeared to depend primarily on the magnitude of the heat flux at the edge of the samples. At the higher heat fluxes, the shells were somewhat shorter than at the lower heat fluxes. Tests in air, of course, resulted in shorter char shells than tests in N_2 and He because of the effects of oxidation. This behavior was also typical of LDPN.

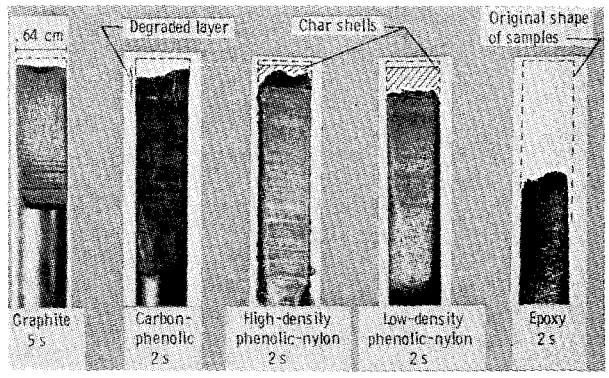

Fig. 6 Cross section of materials after testing in air at 1.0 atm.

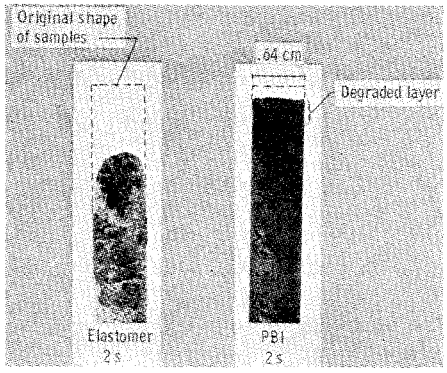

Fig. 7 Elastomer and PBI after testing in air at 0.1 atm.

Figure 6 is a photograph of five samples of various materials after testing in air at 1.0 atm. The total power input to each sample was about 1150 w. The maximum flux density varied from about 44 Mw/m² for the graphite to about 42 Mw/m² for the epoxy sample. The original shape of the samples is indicated by the dashed lines to demonstrate the relative abilities of the materials to withstand the environment. The graphite shows the usual cupping of the front surface resulting from the variation of the heat flux over the surface and, in this case, shows slight material recession at the edge. Graphite tested in N_2 and He showed negligible recession at the edges.

The carbon-phenolic material exhibited considerable cracking and spalling. When the samples were suddenly exposed to the laser beam, sizable pieces of material were ejected, apparently because of internal thermal stresses. In 12 of 14 tests, pieces of material flew off the sample with such force that the NaCl entrance window in the test chamber was coated with it and thus began absorbing heat rapidly from the laser beam and ultimately failed. The window failed in less than 0.5 sec from the start of the tests. The test data were therefore of little value. The carbon-phenolic in the uncharred state has a black, carbon-like appearance, and it absorbs the initial radiation very rapidly; differences in thermal expansion characteristics of the carbon fibers, the phenolic, and the carbon formed by decomposition of the phenolic contribute to the thermal stresses. For the tests in which no spallation occurred, the surfaces of the carbon-phenolic were cupped similar to the graphite samples. However, the material was typically degraded 2–3 mm.

Some spallation of the phenolic-nylon chars was observed, but it was slight and was due to the fact that the char shells that developed were very thin and easily broken. The epoxy material developed very little char as the surface eroded very rapidly in the test environment. Any char that formed during the tests was quickly burned away.

Samples of the elastomeric material and the PBI are shown in Fig. 7. The elastomer experienced very rapid surface recession as well as a significant amount of bending caused by differential thermal expansion within the sample. Surface recession rates were comparable to those of the epoxy material. The elastomer, however, was developed primarily for low-heat flux environments such as may be encountered in entry into Mars[7] and was not expected to perform well in the present experiment.

In the two environments in which it was tested, the PBI performed better than any of the materials except graphite. It developed a substantial thickness of char over the entire front surface of the sample. It was, however, subject to some mechanical removal of the surface material.

Ablative Effectiveness

Quantitatively, the materials were evaluated by an effectiveness parameter based on the measured depth of material degradation at the point of maximum heating. The effectiveness parameter $\bar{E}$ is defined as $\bar{E} = (q_{net})t/\rho\Delta L$ where q_{net} is defined as the measured heat input (energy/unit, time/unit area) minus the heat reradiated at the point of maximum heating, t is the test time, ρ is the uncharred material density, and ΔL is the thickness of material degraded. The heat reradiated is computed from the sublimation temperature of graphite at various pressures as inferred from Refs. 8 and 9. The emittance of all the test materials in the charred state is taken as 0.9 (Ref. 10).

The results for the ablative materials are given in Figs. 8 and 9, where the effectiveness is plotted against chamber pressure and the net heat flux. Data are shown for all test gases considered. For a given material, the performance is relatively insensitive to changes in test gas, chamber pressure, or heat flux over the range considered. There are, however, substantial differences in the behavior of the different materials. The elastomer and the epoxy showed large surface recession rates and hence low values for the effectiveness (about half that of phenolic-nylon). It appears that because of this excessive surface recession, these two materials are not suitable for thermal protection in environments with heat fluxes comparable to those of planetary entry.

The phenolic-nylon and the PBI withstood the environment reasonably well, with the PBI having the largest $\bar{E}$ value of any material, other than graphite, in the two environments in which it was tested. It is of some significance that the lower density ablators (i.e., LDPN and PBI) showed the best performance. The low-density materials are, in general, good insulators, and a requirement for lightweight heat shields is that the material be a good insulator as well as an efficient ablator. Therefore, it appears that some presently available charring ablators could be used as effective and efficient thermal protection systems for planetary missions.

Figure 10 shows the effectiveness of graphite as a function of heat flux. Data are shown for the three test gases and the three pressures considered. The values of $\bar{E}$ for the air tests are considerably lower than those for the N_2 and He tests. This behavior is most likely caused by combustion of carbon

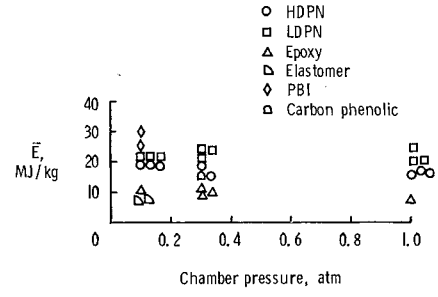

Fig. 8 Effect of pressure on effectiveness of ablative materials.

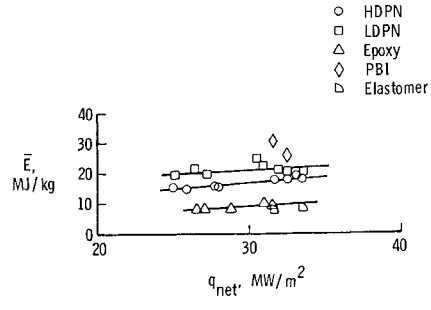

Fig. 9 Effect of heat flux on effectiveness of ablative materials.

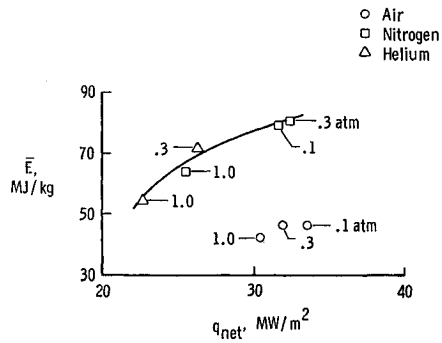

Fig. 10 Effect of heat flux on effectiveness of graphite.

in the hot gas layer adjacent to the sample surface, which causes an additional heat input to the sample resulting in increased mass loss and, hence, reduced effectiveness. There was little effect of pressure on the graphite performance in air.

For the N_2 and He tests, it is difficult to separate the effects of the test variables, but $\bar{E}$ may have been affected more by changes in heat flux than by changes in pressure. For example, tests in He should result in larger values of $\bar{E}$ for a given pressure and heat flux, since sublimation is the only means by which material is removed; but Fig. 10 shows that for a given pressure, $\bar{E}$ for the N_2 tests is somewhat greater than that for the He tests. However, the heat flux for N_2 is also greater than that for He at the same pressure. In addition, graphite tests in N_2 at 0.1 and 0.3 atm, at about the same heat flux, resulted in essentially the same effectiveness. Also, the difference in $\bar{E}$ was small for tests in N_2 at 1.0 atm and in He at 0.3 atm, indicating that the graphite behaved similarly in N_2 and He.

The increase in effectiveness with increasing heat flux could be caused by additional absorption of the incident energy by the ablative products. That is, an increase in heat flux causes a corresponding increase in mass loss rate and hence a greater amount of ablative gases is produced which, in turn, absorbs a greater amount of the incident energy.

In general, the graphite performed much as expected. If the equilibrium value for the heat of sublimation at 1.0 atm pressure (28 Mjoule/kg) is used, and the heat required to raise the material to its sublimation temperature is considered, then the theoretical value of $\bar{E}$ is about 41 Mjoule/kg. This value should be the same as that for the helium test at 1.0 atm if heat is dissipated by sublimation only. It is reasonably close to the experimental value of 55 Mjoule/kg when it is recognized that in the present calculation the heat losses from conduction through the material, absorption of radiation by the gas cap, and radiation from the sample sides have not been considered.

Concluding Remarks

Seven ablative materials were subjected to very high radiative heat fluxes in controlled atmospheres at pressures of 0.1, 0.3, and 1.0 atm. The radiative environment, 36–47 Mw/m^2, was produced by a 9-kw, continuous-wave CO_2 laser. For the ablative materials, an effectiveness parameter based on the heat input to the sample and the mass of material degraded was relatively insensitive to test gas, pressure, or the level of heat flux over the range considered. A carbon-phenolic material experienced considerable spallation. Elastomeric and epoxy materials showed excessive surface recession and appeared to be unsatisfactory for such high-heat flux environments. The PBI and phenolic-nylon performed satisfactorily, with the PBI showing the largest value of ablative effectiveness of any materials except graphite in the two environments in which it was tested.

In N_2 and He atmospheres, the effectiveness of graphite increased with increasing heat flux over the range considered, but its effectiveness in air was considerably lower; chamber pressure had little effect on its performance in any of the test gases.

References

[1] Swann, R. T., Pittman, C. M., and Smith, J. C., "One-Dimensional Numerical Analysis of the Transient Response of Thermal Protection Systems," TN D-2976, 1965, NASA.

[2] Anderson, J. D., Jr., "An Engineering Survey of Radiating Shock Layers," AIAA Paper 68-1151, Williamsburg, Va., 1968.

[3] Horrigan, F. A. et al., "High Power Gas Laser Research," Final Technical Rept. Contract DA-AHol 67-1589, Sept. 1968, Raytheon Research Div., Waltham, Mass.

[4] Wilson, R. G., "Thermophysical Properties of Six Charring Ablators From 140° to 700°K and Two Chars From 800° to 3000°K," TN D-2991, 1965, NASA.

[5] Swann, R. T., Brewer, W. D., and Clark, R. K., "Effect of Composition, Density, and Environment on the Ablative Performance of Phenolic Nylon," TN D-3908, 1967, NASA.

[6] Dickey, R. R., Lundel, J. H., and Parker, J. A., "The Development of Polybenzimidazole Composites as Ablative Heat Shields," *Journal of Macromolecular Science-Chemistry*, Vol. A3, No. 4, July 1969, pp. 573–584.

[7] Vosteen, L. F., "Heat Shield Materials Development for Voyager," Presented at Third International Symposium on High Temperature Technology, Asilomar, Pacific Grove, Calif., Sept. 17–20, 1967.

[8] Glocker, G., *Journal of Chemistry and Physics*, Vol. 22, 1954, p. 159.

[9] Zavitzanos, P. D., "Mass Spectrometric Analysis of Carbon Species Generated by Laser Evaporation," *Carbon 1968*, Vol. 6, 1968, pp. 731–737.

[10] Wilson, R. Gale, "Hemispherical Spectral Emittance of Ablation Chars, Carbon, and Zirconia to 3700° K," TN D-2704, 1965, NASA.